

## Critical behavior of two-dimensional spin systems under the random-bond six-state clock model

Raymond P. H. Wu, Veng-cheong Lo, and Haitao Huang

Citation: *J. Appl. Phys.* **112**, 063924 (2012); doi: 10.1063/1.4754821

View online: <http://dx.doi.org/10.1063/1.4754821>

View Table of Contents: <http://jap.aip.org/resource/1/JAPIAU/v112/i6>

Published by the [American Institute of Physics](#).

---

### Related Articles

The role of dipole-dipole interaction in modulating the step-like magnetization of  $\text{Ca}_3\text{Co}_2\text{O}_6$

*J. Appl. Phys.* **111**, 07E133 (2012)

Dipolar ordering of random two-dimensional spin ensemble

*Appl. Phys. Lett.* **100**, 052406 (2012)

A study of the dielectric and magnetic properties of multiferroic materials using the Monte Carlo method

*AIP Advances* **2**, 012122 (2012)

Evidence for low-temperature antiferromagnetic phase transition in Ising singlet magnet  $\text{KTb}(\text{WO}_4)_2$

*Low Temp. Phys.* **37**, 1048 (2011)

Critical properties of an antiferromagnetic Ising model on a square lattice with interactions of the next-to-nearest neighbors

*Low Temp. Phys.* **37**, 1001 (2011)

---

### Additional information on *J. Appl. Phys.*

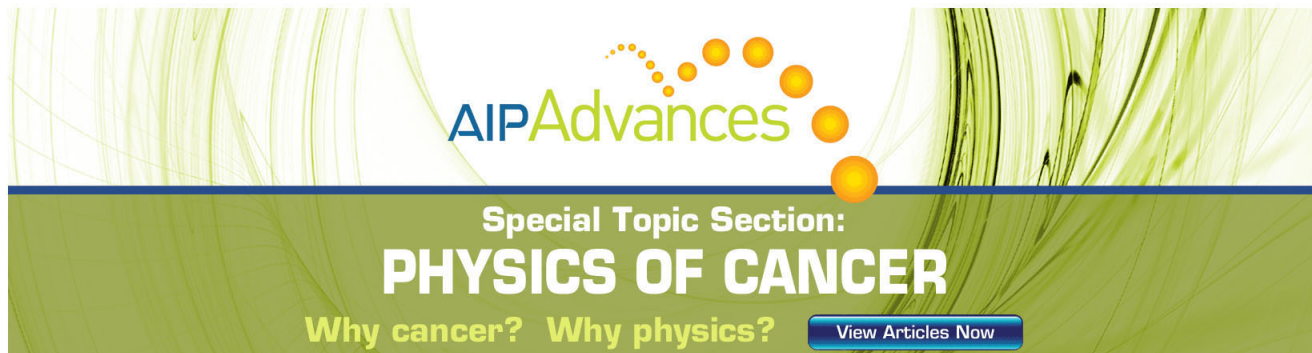
Journal Homepage: <http://jap.aip.org/>

Journal Information: [http://jap.aip.org/about/about\\_the\\_journal](http://jap.aip.org/about/about_the_journal)

Top downloads: [http://jap.aip.org/features/most\\_downloaded](http://jap.aip.org/features/most_downloaded)

Information for Authors: <http://jap.aip.org/authors>

## ADVERTISEMENT



**AIP Advances**

Special Topic Section:  
**PHYSICS OF CANCER**

Why cancer? Why physics? [View Articles Now](#)

## Critical behavior of two-dimensional spin systems under the random-bond six-state clock model

Raymond P. H. Wu,<sup>a)</sup> Veng-cheong Lo, and Haitao Huang

*Department of Applied Physics, The Hong Kong Polytechnic University, Hung Hom, Kowloon, Hong Kong*

(Received 28 March 2012; accepted 24 August 2012; published online 27 September 2012)

The critical behavior of the clock model in two-dimensional square lattice is studied numerically using Monte Carlo method with Wolff algorithm. The Kosterlitz-Thouless (KT) transition is observed in the six-state clock model, where an intermediate phase exists between the low-temperature ordered phase and the high-temperature disordered phase. The bond randomness is introduced to the system by assuming a Gaussian distribution for the coupling coefficients with the mean  $\mu = 1$  and different values of variance, from  $\sigma^2 = 0.1$  to  $\sigma^2 = 3.0$ . An abrupt jump in the helicity modulus at the transition, which is the key characteristic of the KT transition, is verified with a stability argument. The critical temperature  $T_c$  for both pure and disordered systems is determined from the critical exponent  $\eta(T_c) = 1/4$ . The results showed that a small amount of disorder (small  $\sigma$ ) reduces the critical temperature of the system, without altering the nature of transition. However, a larger amount of disorder changes the transition from the KT-type into that of non-KT-type. © 2012 American Institute of Physics. [<http://dx.doi.org/10.1063/1.4754821>]

### I. INTRODUCTION

In statistical mechanics, ferromagnetic systems can be described by various spin models such as the Ising model<sup>1,2</sup> and the Potts model.<sup>3</sup> In a ferromagnetic system, non-zero magnetization is developed below a critical temperature  $T_c$ . As the temperature increases above  $T_c$ , the magnetization becomes zero and the system becomes paramagnetic. If the system is cooled down again, just below  $T_c$ , the ferromagnetic phase recurs again. The transition from paramagnetic phase to ferromagnetic phase is determined by the competition between the spin-spin interactions and the thermal fluctuations acting on the system. In these systems, spontaneous symmetry breaking occurred and long-range order is developed at the transition. The phase transition is of great interest, because there is universality in the critical phenomena. At the transition, the details of the physical system are not important and the properties of the system are only governed by the critical exponents. Different models with the same critical exponents are said to belong to the same universality class. It happens that, a single model, elaborated to study certain phenomenon is found to be useful in studying another physical situation with the same universality class. Most phase transitions, including those exhibited by the Ising model and the Potts model belong to either the first-order type or the second-order type.

Apart from the ordinary first-order and second-order phase transitions manifested in most spin models, a specific phase transition called the Kosterlitz-Thouless (KT) transition is observed in superfluid systems and it can be described by the two-dimensional XY model.<sup>4-6</sup> Unlike the phase transitions in other spin models, there are excitations of spin waves and vortices in the XY model. The driving force behind the KT transition involves the binding and unbinding

of the vortex-antivortex pairs, which play the role of charges in the system. This is entirely different from the simple spin-spin interactions in other spin models. The KT transition does not involve symmetry breaking and only topological long-range order is found in the system.

The  $q$ -state clock model is a discrete version of the XY model. In this model, an ensemble of spins with  $q$  different orientations interact with each other and the strength of interactions are determined by the coupling coefficients which are usually assumed to be a constant. For  $q = 2$ , the clock model reduces to the Ising model, while for  $q = 3$ , it is equivalent to the three-state Potts model, and for  $q = 4$ , it is also called the Ashkin-Teller model,<sup>7</sup> which is the four-component version of the Ising model. At the limiting case  $q \rightarrow \infty$ , where the spin state varies continuously, it restores to the XY model. It is known that, the phase transition in the Ising model is of the second-order type, while that in the XY model is of the KT-type. The clock model, being a bridge between different models, is expected to have various critical behavior under different values of  $q$ . Extensive studies<sup>8-15</sup> on the clock model had shown that, for  $q \leq 4$ , the phase transition is Ising-like, and for  $q \geq 6$ , it is XY-like. There is still no conclusive result for the case where  $q = 5$ .<sup>9,15-17</sup> Since the critical behavior for the  $q$ -state clock model does not change appreciably on varying  $q$  values when  $q$  is large. This means that, without using the XY model, which involves the continuous spin state, the six-state clock model ( $q = 6$ ) can be used to study the KT transition.

The presence of defects interrupts the periodic structure of crystalline materials and the systems become disordered when the quantity of interruptions is large. It can be visualized by a random distribution of coupling coefficients between neighboring spins. The effects of disorder on phase transition have attracted many interests.<sup>18-20</sup> In some systems, a small amount of disorder can have dramatic effects and even changes the nature of phase transition.<sup>19</sup> A number

<sup>a)</sup>Electronic mail: rayphwu@gmail.com.

of numerical works<sup>21–23</sup> had studied the effects of non-magnetic impurities on the KT transition. Since non-magnetic impurities can be viewed as lattice vacancies, the results found that the KT transition disappears as the vacancy density reaches the lattice percolation limit. In real systems, the source of defects may not be only from the non-magnetic impurities but also from the magnetic ones. In statistical point of view, it is natural to consider a Gaussian distribution for the coupling coefficients. Theoretical works<sup>24</sup> conjectured that strong disorder will induce a first-order phase transition in the XY model. It is our motivation to study the effects of disorder on the phase transition in the six-state clock model.

## II. MODEL

We consider an ensemble of spins on a two-dimensional square lattice with size  $N = L \times L$ . For simplicity, we assumed the spins interact with their nearest neighbors only. In the  $q$ -state clock model, the spins are confined in a plane with  $q$  different orientations each of which is specified by a phase angle

$$\theta_n = n \left( \frac{2\pi}{q} \right), \quad (1)$$

where  $n = 0, 1, 2, \dots, q-1$  denotes the state of a spin. The Hamiltonian of the clock model takes the form  $H = -\sum_{\langle ij \rangle} K(\theta_{ij})$ , where  $\langle ij \rangle$  denotes the summation is over

the nearest neighbors only and  $\theta_{ij} = \theta_i - \theta_j$  is the phase angle difference between two spins at lattice sites  $i$  and  $j$ . The function  $K(\theta)$  is periodic with a period  $2\pi$ . One simple form for  $K(\theta)$  is  $K(\theta) = J \cos \theta$ , where  $J$  is the coupling coefficient between two neighboring spins. The Hamiltonian is then given by

$$H = -\sum_{\langle ij \rangle} J_{ij} \cos(\theta_i - \theta_j). \quad (2)$$

The spin at spin state  $n$  can also be denoted by the spin vector

$$\mathbf{S}_n = (\sin \theta_n, \cos \theta_n). \quad (3)$$

Subsequently, the Hamiltonian can be expressed as

$$H = -\sum_{\langle ij \rangle} J_{ij} \mathbf{S}_i \cdot \mathbf{S}_j. \quad (4)$$

Usually, the coupling coefficients  $J_{ij}$  are assumed to be a constant  $J$ . A positive  $J$  value indicates a ferromagnetic system, where the energy is lowered by aligning the spins in the same direction. On the contrary, a negative  $J$  value makes the neighboring spins oppositely aligned and results in an antiferromagnetic system. To investigate the effects of disorder, the coupling coefficients  $J_{ij}$  are assumed to follow the Gaussian distribution

$$P(J) = \frac{1}{\sqrt{2\pi\sigma^2}} \exp \left[ -\frac{(J - \mu)^2}{2\sigma^2} \right], \quad (5)$$

where  $\mu = 1$  is the mean and  $\sigma^2$  is the variance of the distribution. The bond randomness is reflected by the parameter  $\sigma$ . In particular,  $\sigma^2 = 0$  represents a pure system with no disorder and with constant coupling coefficient  $J = 1$ .

## III. MONTE CARLO ALGORITHM

We performed numerical calculations using Monte Carlo method and the periodic boundary conditions were applied to the lattice with size up to  $N = 128 \times 128$ . The Wolff algorithm<sup>25</sup> which is the improvement of the Swendsen-Wang algorithm,<sup>26</sup> is applicable to many spin models including the clock model. Instead of updating a single spin, a cluster of spins is updated in the Wolff algorithm to overcome the problem of critical slowing down. We adopted the original idea of Wolff which applies to the XY model. The specialized algorithm for the  $q$ -state clock model is described as follows:

- (1) A mirror line is chosen randomly with a normal vector  $\mathbf{r}$ .
- (2) A lattice site  $i$  is chosen randomly for a cluster formation.
- (3) Spins at the neighboring sites  $j$  are added to the cluster according to the probability

$$P = 1 - \exp \left[ -\frac{2J_{ij}}{T} (\mathbf{r} \cdot \mathbf{S}_i)(\mathbf{r} \cdot \mathbf{S}_j) \right]. \quad (6)$$

- (4) The cluster is updated by reflecting all the spins in the line perpendicular to the normal vector  $\mathbf{r}$ .

To implement these procedures, consider the normal vector

$$\mathbf{r}_k = (\sin \phi_k, \cos \phi_k), \quad (7)$$

where the angles  $\phi_k$  specifies the state of the normal vector and for even  $q$

$$\phi_k = k \left( \frac{\pi}{q} \right), \quad (8)$$

while for odd  $q$

$$\phi_k = \left( k + \frac{1}{2} \right) \left( \frac{\pi}{q} \right), \quad (9)$$

where  $k = 0, 1, 2, \dots, 2q-1$ . Then the phase angle of the reflected spin is given by

$$\mathbf{R}\theta = 2\phi - \theta + \pi, \quad (10)$$

where  $\mathbf{R}$  is the reflection operator. Then all the combinations for different spin vectors  $\mathbf{S}_n$  and normal vectors  $\mathbf{r}_k$  can be pre-calculated to reduce the computational cost.

## IV. METHODS

### A. Magnetization, specific heat, and susceptibility

Several properties of the system are calculated in order to study the phase transitions in the clock model. The energy per spin  $E$  of the system is given by

$$E = -\frac{1}{N} \left\langle \sum_{\langle ij \rangle} J_{ij} \mathbf{S}_i \cdot \mathbf{S}_j \right\rangle, \quad (11)$$

where  $\langle \dots \rangle$  denotes the ensemble average of the quantities. The magnetization per spin  $\mathbf{m}$  is given by

$$\mathbf{m} = \left( \left\langle \frac{1}{N} \sum_i \sin \theta_i \right\rangle, \left\langle \frac{1}{N} \sum_i \cos \theta_i \right\rangle \right), \quad (12)$$

and its magnitude is represented by  $m$ . Furthermore, the specific heat per spin  $c$  can be obtained from the fluctuations of energy and is given by

$$c = \frac{1}{k_B T^2} (\langle E^2 \rangle - \langle E \rangle^2). \quad (13)$$

Similarly, the susceptibility per spin  $\chi$  is given by

$$\chi = \frac{N}{k_B T} (\langle m^2 \rangle - \langle m \rangle^2). \quad (14)$$

## B. Helicity modulus and fourth-order helicity modulus

Besides judging the existence of the KT transition from the above properties of the system, the more convincing evidence is by observing the critical behavior of the helicity modulus. Consider the Hamiltonian of the clock model including an externally imposed spin twist  $\Delta = (\Delta_x, \Delta_y)$  across the system

$$H = - \sum_{\langle ij \rangle} J_{ij} \cos(\theta_i - \theta_j - \frac{1}{L} \mathbf{r}_{ij} \cdot \Delta), \quad (15)$$

where  $\mathbf{r}_{ij}$  is a unit vector pointing from lattice site  $i$  to  $j$ . The components of the spin twist  $\Delta_x$  and  $\Delta_y$  are defined by the summation of the phase angle difference  $\theta_{ij}$  along the  $\mathbf{x}$  and  $\mathbf{y}$  directions, respectively. The helicity modulus per spin  $\Upsilon$  is a measure of the resistance to an infinitesimal spin twist across the system along one direction. It is related to the free energy per spin  $F$  of the system by  $\Upsilon \equiv \partial^2 F / \partial \Delta^2 |_{\Delta=0}$ , which leads to the expression

$$\Upsilon = -\frac{1}{2} \langle E \rangle - \frac{N}{T} \langle s^2 \rangle, \quad (16)$$

where

$$s \equiv \frac{1}{N} \sum_{\langle ij \rangle} J_{ij} \sin(\theta_i - \theta_j) (\mathbf{r}_{ij} \cdot \mathbf{x}). \quad (17)$$

According to the renormalization group calculations,<sup>5</sup> the helicity modulus in the  $XY$  model which undergoes the KT transition jumps from the value  $(2/\pi)T_c$  to zero at the transition in the thermodynamic limit. This abrupt jump in the helicity modulus at the transition is the key feature of the KT transition. Unfortunately, it is very difficult to determine the discontinuity of the helicity modulus from numerical calculations because of the limited precision.

A new numerical method<sup>27</sup> based on a stability argument can be used to identify the KT transition. The expansion of free energy of the system gives  $F(\Delta) = \langle \Upsilon \rangle \frac{\Delta^2}{2} + \langle \Upsilon_4 \rangle \frac{\Delta^4}{4!} + \dots$ , where  $\Upsilon_4 \equiv \partial^4 F / \partial \Delta^4 |_{\Delta=0}$  is the fourth-order helicity modulus and it can be expressed as

$$\begin{aligned} \langle \Upsilon_4 \rangle = & \frac{1}{2N} \langle E \rangle + \frac{3}{4T} \langle E \rangle^2 - \frac{3}{4T} \langle E^2 \rangle + \frac{4}{T} \langle s^2 \rangle + \frac{3N^2}{T^3} \langle s^2 \rangle^2 \\ & + \frac{3N}{T^2} \langle E \rangle \langle s^2 \rangle. \end{aligned} \quad (18)$$

A spin twist to the system gives an additional contribution to the free energy so that  $F(\Delta) \geq F(0)$ . Since the helicity modulus  $\Upsilon$  must be non-negative and in the  $XY$  model, this quantity is positive and finite below the critical temperature and is zero above it. Consequently, the fourth-order helicity modulus  $\Upsilon_4$  must also be non-negative at any temperature where  $\Upsilon$  vanishes. Supposed  $\Upsilon_4$  is negative at the transition, then  $\Upsilon$  cannot approach zero continuously but must make a discontinuous jump to zero at the transition instead. Hence, we can distinguish the KT transition from the ordinary first-order or the second-order phase transition by the fourth-order helicity modulus.

## C. Critical exponent and critical temperature

From the theory developed by Kosterlitz,<sup>5</sup> it is known that at  $T \rightarrow T_c$ , the correlation length  $\xi$  and the susceptibility  $\chi$  in the  $XY$  model diverge according to the asymptotic laws

$$\xi \propto \exp(bt^{-1/2}), \quad (19)$$

where  $t \equiv (T - T_c)/T_c$  and  $b \approx 1.5$ , and

$$\chi \propto \xi^{2-\eta}, \quad (20)$$

where the critical exponent  $\eta = 1/4$  has the same value as that of the two-dimensional Ising model<sup>2</sup> and is the only exponent in the absence of external field for the  $XY$  model. From the studies of the superfluid systems,<sup>6</sup> the helicity modulus is given by  $\Upsilon = (\hbar/m)^2 \rho_s$ , where  $m$  is the mass of the superfluid and  $\rho_s$  is density of the superfluid. The critical exponent is given by  $\eta = (T/2\pi)(\hbar/m)^2 \rho_s$ . Then we can obtain a relation

$$\eta = \frac{T}{2\pi \Upsilon}. \quad (21)$$

Hence, the critical exponent  $\eta$  can be calculated from the helicity modulus  $\Upsilon$ . This, in turn, enables us to determine the critical temperature  $T_c$  from the point where the critical exponent  $\eta(T_c) = 1/4$ . Furthermore, since the helicity modulus  $\Upsilon$  jumps from the value  $(2/\pi)T_c$  to zero at the transition, we can also determine the critical temperature  $T_c$  from the intersection of the curve and the straight line

$$\Upsilon = \frac{2}{\pi} T. \quad (22)$$

## V. RESULTS AND DISCUSSION

### A. Second-order phase transition and the KT transition

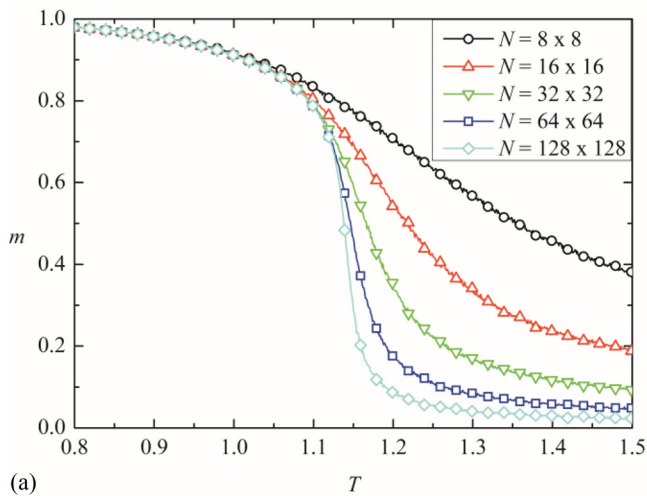
The four-state clock model ( $q = 4$ ) is known to be equivalent to the Ising model ( $q = 2$ ). The nature of phase transitions for both cases is essentially the same, being of the second-order type. On the other hand, the phase transition in the six-state clock model ( $q = 6$ ) is known to be of the KT-type. Several properties of the clock model with  $q = 4$  and  $q = 6$  are calculated under the same conditions to demonstrate the differences between the second-order phase transition and the KT transition in these models.

The magnetization against temperature for the four-state and the six-state clock model with various lattice sizes are given in Figs. 1(a) and 1(b), respectively. In the four-state clock model, the magnetization is non-zero below the critical temperature and above which it vanishes. The low-temperature ordered phase and the high-temperature disordered phase are separated at the critical temperature, manifesting the second-order phase transition. However, in the six-state clock model, the magnetization undergoes two transitions instead of a single one. There exists an inter-

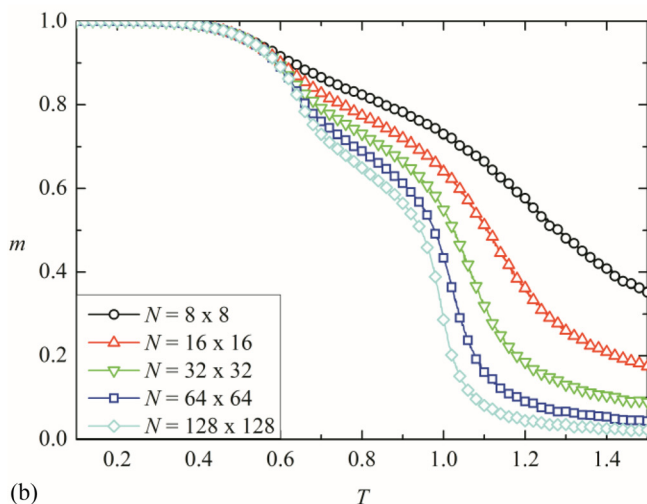
mediate phase called the KT phase (or the massless phase) between the low-temperature ordered phase and the high-temperature disordered phase.

The specific heat against temperature for the four-state and the six-state clock model with various lattice sizes are given in Figs. 2(a) and 2(b), respectively. Also, the susceptibility against temperature for the four-state and the six-state clock model with various lattice sizes are given in Figs. 3(a) and 3(b), respectively. In the four-state clock model, a single peak emerges in both specific heat and susceptibility. They diverge at the critical temperature as expected in the second-order phase transition. On the other hand, double peaks are observed in the six-state clock model. Again, this is a manifestation of the KT transition. It is found that, in both cases, as the size of the lattice increases, the peaks of both specific heat and susceptibility become sharper. In the four-state clock model, the critical temperature decreases as the lattice size increases. In the six-state clock model, the upper critical temperature also decreases as the lattice size increases, but there is no appreciable effect on the lower critical temperature.

The helicity modulus against temperature for the four-state and the six-state clock models with various lattice sizes are given in Figs. 4(a) and 4(b), respectively. In the

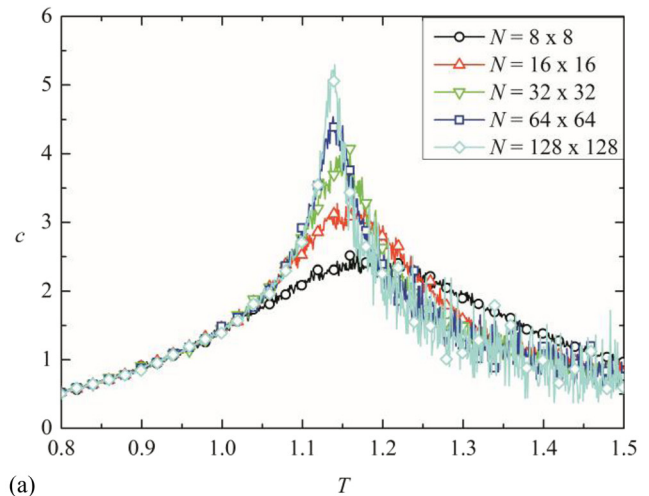


(a)

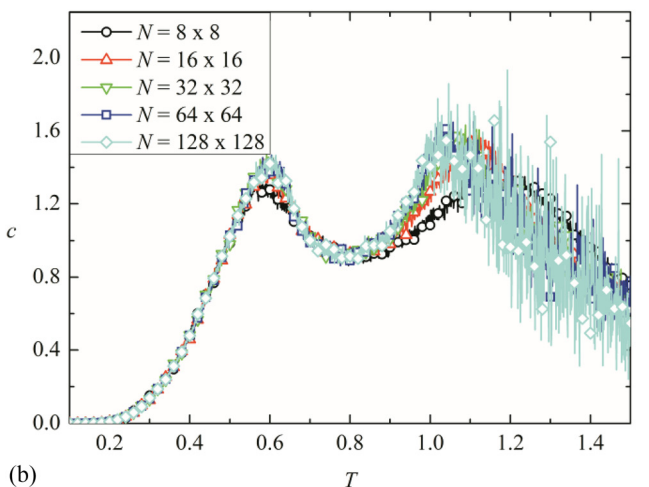


(b)

FIG. 1. The magnetization against temperature for (a) the four-state clock model and (b) the six-state clock model with various lattice sizes.

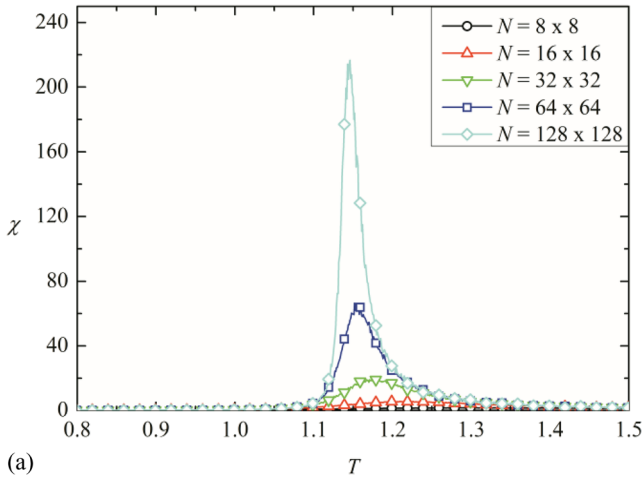


(a)

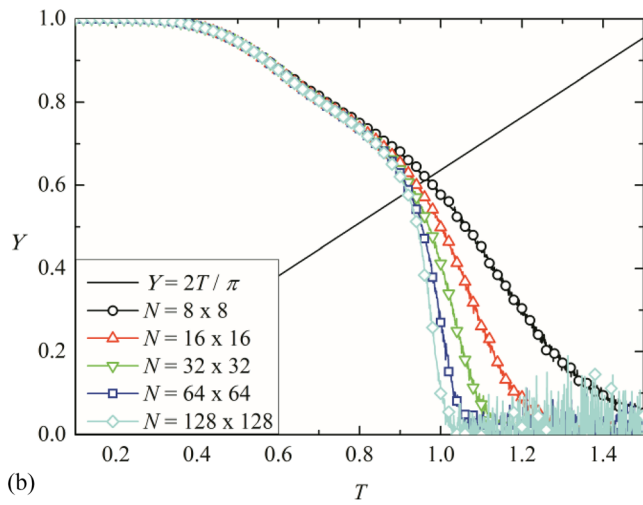


(b)

FIG. 2. The specific heat against temperature for (a) the four-state clock model and (b) the six-state clock model with various lattice sizes.



(a)



(b)

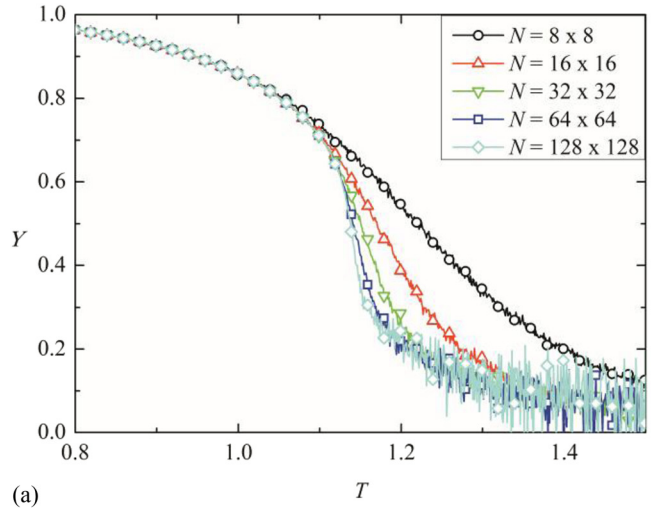
FIG. 3. The susceptibility against temperature for (a) the four-state clock model and (b) the six-state clock model with various lattice sizes.

four-state clock model, the helicity modulus remains positive and finite across the transition despite the finite-size effect. However, in the six-state clock model, it vanishes above the critical temperature. In order to demonstrate an abrupt jump in the helicity modulus in the six-state clock model, the fourth-order helicity modulus against temperature with various lattice sizes is given in Fig. 5. It is demonstrated that the fourth-order helicity modulus is negative at the phase transition and thus the discontinuous nature of the helicity modulus is confirmed. Hence, the phase transition for the six-state clock model is of the KT-type.

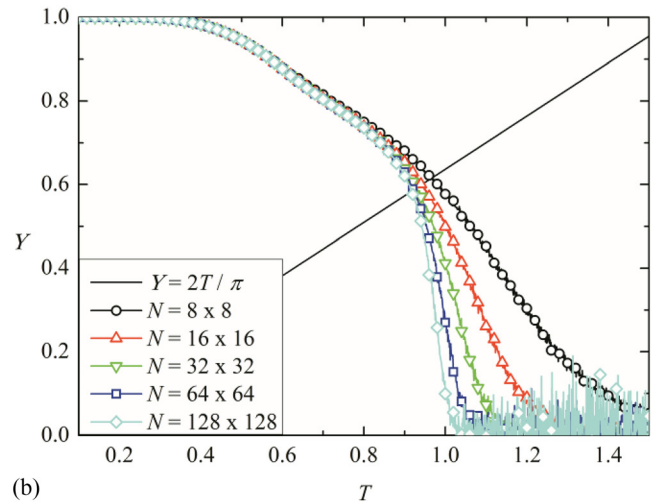
The critical exponent  $\eta$  against temperature for the six-state clock model with various lattice sizes is given in Fig. 6. The critical temperature that determined from the critical exponent  $\eta$  and from the helicity modulus are the same. The results are given in Table I. For the largest lattice size  $N = 128 \times 128$ , the critical temperature is  $T_c = 0.916$ , which is consistent with the literatures.<sup>8–12,14</sup>

**B. Random-bond six-state clock model**

From the above results, the KT transition in the pure six-state clock model has been demonstrated. Subsequently, the effects of disorder on the phase transition in the six-state



(a)



(b)

FIG. 4. The helicity modulus against temperature for (a) the four-state clock model and (b) the six-state clock model with various lattice sizes.

clock model are then investigated. The bond randomness is reflected by the parameter  $\sigma$  as defined in Eq. (5). The results with lattice size  $N = 128 \times 128$  and with different values of  $\sigma$  are shown as follows.

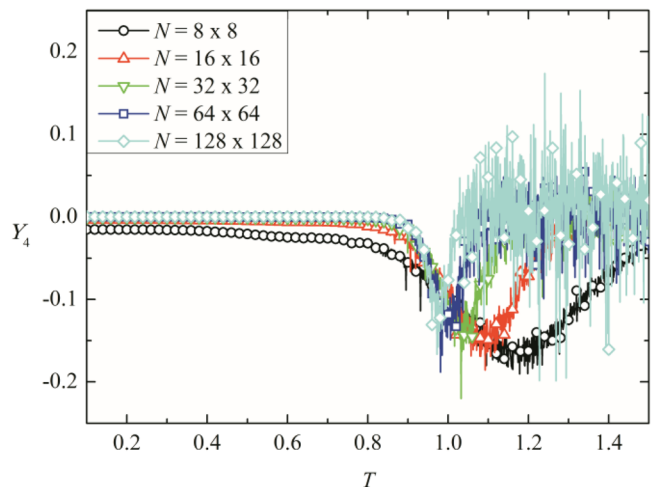


FIG. 5. The fourth-order helicity modulus against temperature for the six-state clock model with various lattice sizes.

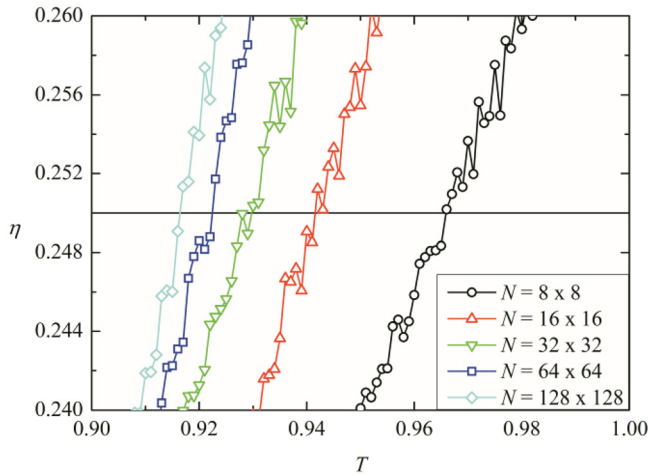


FIG. 6. The critical exponent  $\eta$  against temperature for the six-state clock model with various lattice sizes.

The magnetization against temperature for the random-bond six-state clock model with various  $\sigma^2$  is given in Fig. 7. As  $\sigma$  increases, the critical temperature of the system decreases. In the pure system, there exists an intermediate phase between the low-temperature ordered phase and the high-temperature disordered phase. However, as  $\sigma$  increases, this intermediate phase reduces and for  $\sigma^2 = 3.0$ , it becomes unobservable. In this case, the critical behavior of the magnetization looks very similar to that of the four-state clock model.

The specific heat and the susceptibility against temperature for the random-bond six-state clock model with various  $\sigma^2$  are given in Figs. 8 and 9, respectively. The results for the specific heat are very noisy especially for large  $\sigma$ . However, we can still able to identify the double-peak feature as in the pure system for small  $\sigma$ . The results for the susceptibility are much clearer and again the double-peak feature emerges. As  $\sigma$  increases, all the peaks of both specific heat and susceptibility shift to the left, indicating the decreases in the critical temperature. The distance between the two peaks in the susceptibility decreases as  $\sigma$  increases and for  $\sigma^2 = 3.0$ , they merge together as one. Furthermore, the height of the peak increases as  $\sigma$  increases and for  $\sigma^2 = 3.0$ , it becomes comparable with that of the four-state clock model.

The above results for the random-bond six-state clock model showed the shrinkage of the intermediate phase as the amount of disorder ( $\sigma$ ) increases. Under a large amount of disorder, the phase transition seems to be of the second-order type as in the four-state clock model. The intermediate phase

TABLE I. The critical temperature for the six-state clock model with various lattice sizes.

$N$	$T_c$
$8 \times 8$	0.966
$16 \times 16$	0.942
$32 \times 32$	0.930
$64 \times 64$	0.922
$128 \times 128$	0.916

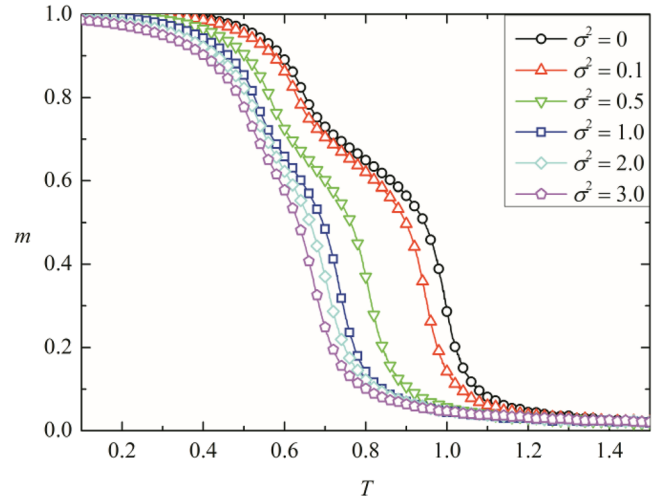


FIG. 7. The magnetization against temperature for the random-bond six-state clock model with lattice size  $N = 128 \times 128$  and various  $\sigma^2$ .

disappeared and only the low-temperature ordered phase and the high-temperature disordered phase are observed. In order to demonstrate the disappearance of the KT transition under a large amount of disorder, the helicity modulus and the fourth-order helicity modulus of the system are calculated. The helicity modulus against temperature for the random-bond six-state clock model with various  $\sigma^2$  is given in Fig. 10. As  $\sigma$  increases, the transition becomes boarder. The helicity modulus still vanishes above the critical temperature for large  $\sigma$ . However, it tends to be continuous rather than makes a discontinuous jump at the transition. The fourth-order helicity modulus against temperature for the random-bond six-state clock model with various  $\sigma^2$  is given in Fig. 11. For  $\sigma^2 = 0.1$  and  $\sigma^2 = 0.5$ , the fourth-order helicity modulus at the transition are clearly negative, implying the system undergoes the KT transition. However, despite the noisy nature, the depth of the trough reduces as  $\sigma$  increases. For  $\sigma^2 = 3.0$ , the trough is no longer observable and thus the helicity modulus does not jump discontinuously. Hence we

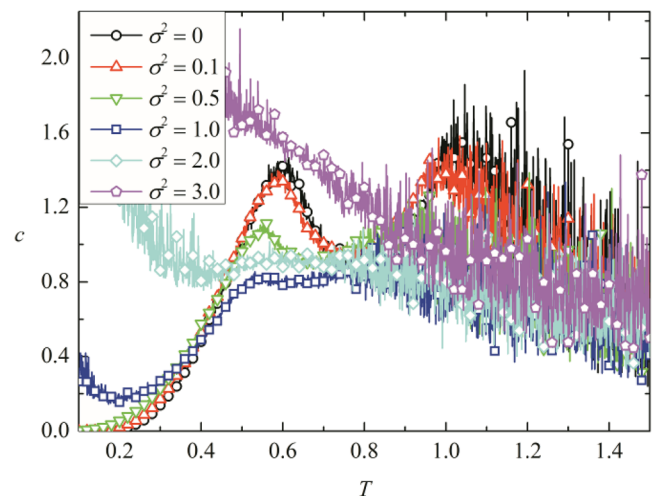


FIG. 8. The specific heat against temperature for the random-bond six-state clock model with lattice size  $N = 128 \times 128$  and various  $\sigma^2$ .

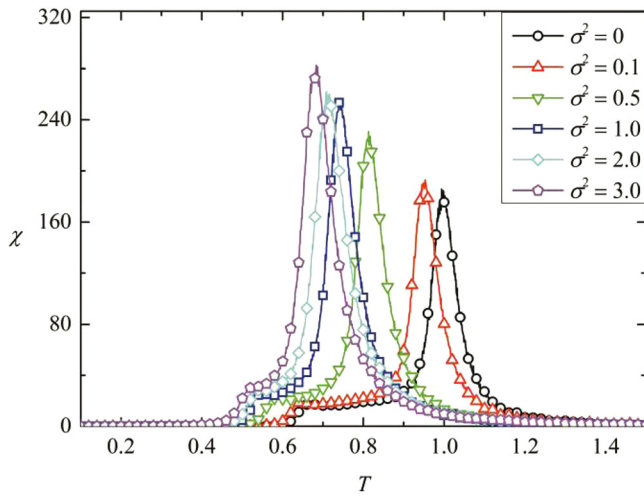


FIG. 9. The susceptibility against temperature for the random-bond six-state clock model with lattice size  $N = 128 \times 128$  and various  $\sigma^2$ .

can conclude that the transition is no longer of the KT-type and this is consistent with our observations discussed before.

The critical exponent  $\eta$  against temperature for the random-bond six-state clock model with various  $\sigma^2$  is given in Fig. 12. Again, the critical temperature that determined from the critical exponent  $\eta$  and from the helicity modulus are the same. The results are given in Table II. Also, the critical temperature against  $\sigma^2$  for the random-bond six-state clock model is given in Fig. 13. Since the transition is no longer of the KT-type for large  $\sigma$ , the critical temperature determined from these methods may be beyond the definitions described above. Hence the results for  $\sigma^2 = 2.0$  and  $\sigma^2 = 3.0$  are only for comparison purpose.

The driving force behind the KT transition involves the binding and unbinding of the vortex-antivortex pairs. Since these processes are not affected by a small perturbation on the local spin phase angle, under a small amount of disorder, the phase transition is still of the KT-type. However, the binding and unbinding of the vortex-antivortex pairs are prohibited under a large amount of disorder and thus the transi-

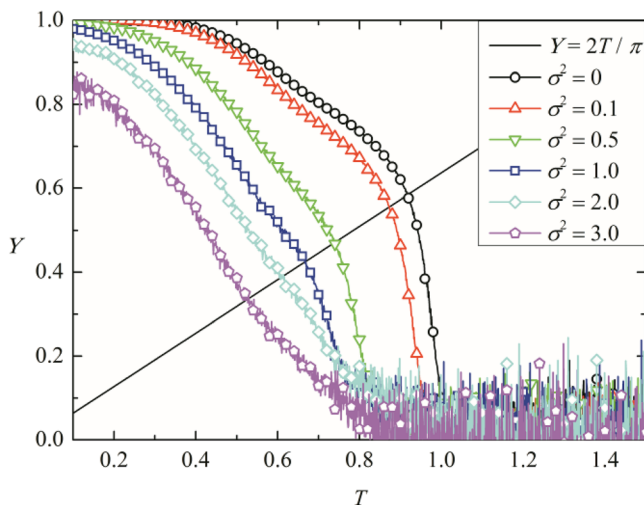


FIG. 10. The helicity modulus against temperature for the random-bond six-state clock model with lattice size  $N = 128 \times 128$  and various  $\sigma^2$ .

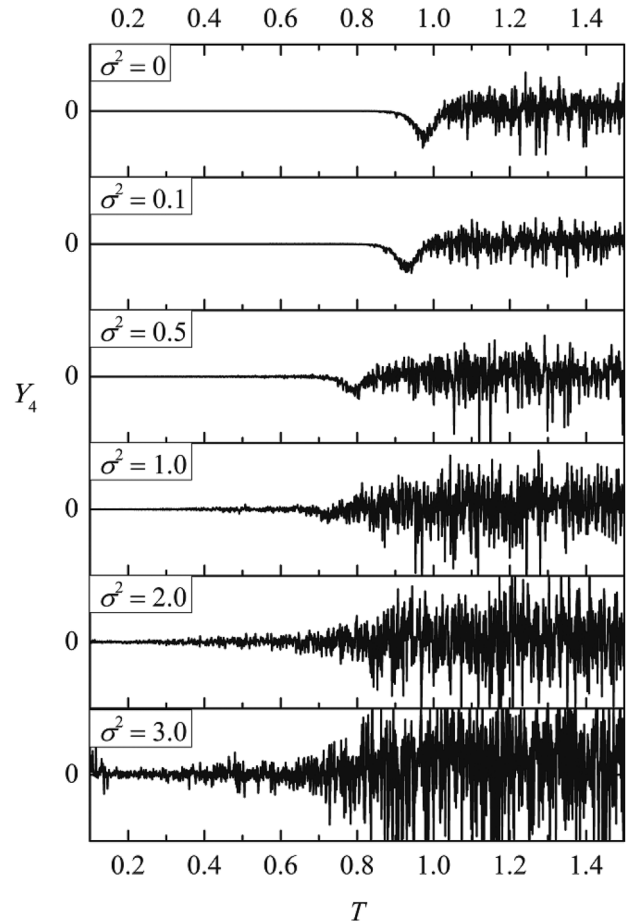


FIG. 11. The fourth-order helicity modulus against temperature for the random-bond six-state clock model with lattice size  $N = 128 \times 128$  and various  $\sigma^2$ .

tion is only determined by the competition between the spin-spin interactions and the thermal fluctuations acting on the system. Hence, the transition is no longer of the KT-type and becomes the ordinary first-order or the second-order phase transition. If the amount of disorder is too large, there will be no phase transition in the system, because the ordering of spins cannot be developed.

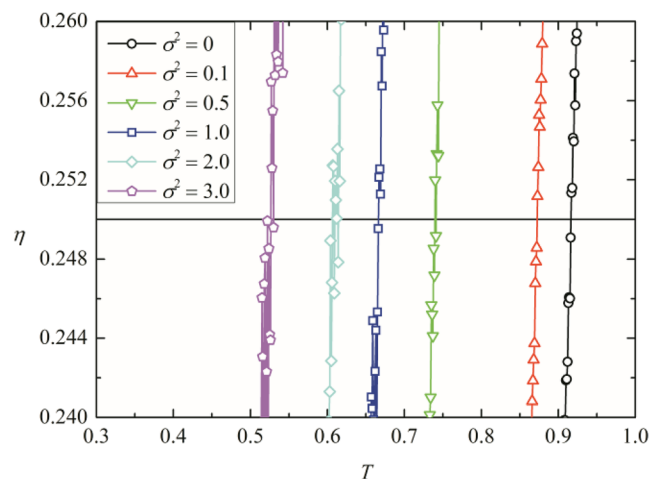
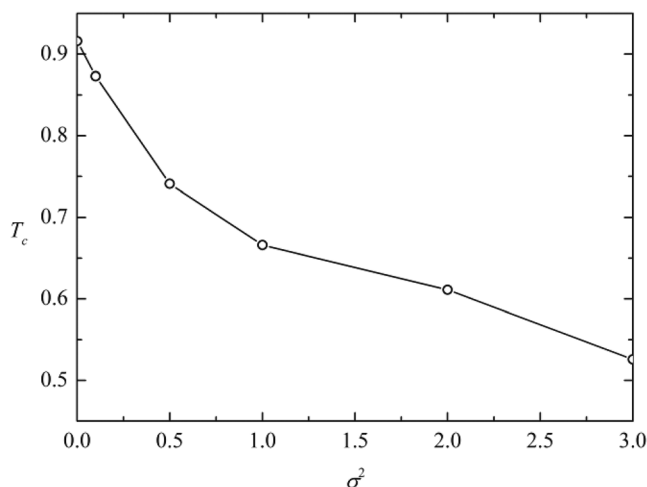


FIG. 12. The critical exponent  $\eta$  against temperature for the random-bond six-state clock model with lattice size  $N = 128 \times 128$  and various  $\sigma^2$ .

TABLE II. The critical temperature for the random-bond six-state clock model with lattice size  $N = 128 \times 128$  and various  $\sigma^2$ .

$\sigma^2$	$T_c$
0	0.916
0.1	0.873
0.5	0.741
1.0	0.666
2.0	0.611
3.0	0.526

FIG. 13. The critical temperature against  $\sigma^2$  for the random-bond six-state clock model with lattice size  $N = 128 \times 128$ .

## VI. CONCLUSION

We have studied the effects of disorder on the phase transition in the six-state clock model ( $q = 6$ ). The critical temperature for both pure and disordered systems is determined. The results showed that a small amount of disorder reduces the critical temperature of the system, without altering the nature of transition. However, a larger amount of dis-

order changes the transition from the KT-type into that of non-KT-type. In the present work, we cannot conclude whether the phase transition of the random-bond six-state clock model changes to the first-order type or the second-order type. Further investigation is necessary.

## ACKNOWLEDGMENTS

This work is financially supported by the research grant from The Hong Kong Polytechnic University under research Grant No. RPRK.

- <sup>1</sup>L. Onsager, *Phys. Rev.* **65**, 117 (1944).
- <sup>2</sup>B. Kaufman and L. Onsager, *Phys. Rev.* **76**, 1244 (1949).
- <sup>3</sup>F. Y. Wu, *Rev. Mod. Phys.* **54**, 235 (1982).
- <sup>4</sup>J. M. Kosterlitz and D. J. Thouless, *J. Phys. C* **6**, 1181 (1973).
- <sup>5</sup>J. M. Kosterlitz, *J. Phys. C* **7**, 1046 (1974).
- <sup>6</sup>D. R. Nelson and J. M. Kosterlitz, *Phys. Rev. Lett.* **39**, 1201 (1977).
- <sup>7</sup>J. Ashkin and E. Teller, *Phys. Rev.* **64**, 178 (1943).
- <sup>8</sup>S. Miyashita, H. Nishimori, A. Kuroda, and M. Suzuki, *Prog. Theor. Phys.* **60**, 1669 (1978).
- <sup>9</sup>J. Tobochnik, *Phys. Rev. B* **26**, 6201 (1982).
- <sup>10</sup>M. S. S. Challa and D. P. Landau, *Phys. Rev. B* **33**, 437 (1986).
- <sup>11</sup>A. Yamagata and I. Ono, *J. Phys. A* **24**, 265 (1991).
- <sup>12</sup>Y. Tomita and Y. Okabe, *Phys. Rev. B* **65**, 184405 (2002).
- <sup>13</sup>C. O. Hwang, *Phys. Rev. E* **80**, 042103 (2009).
- <sup>14</sup>S. K. Baek, P. Minnhagen, and B. J. Kim, *Phys. Rev. E* **81**, 063101 (2010).
- <sup>15</sup>S. K. Baek and P. Minnhagen, *Phys. Rev. E* **82**, 031102 (2010).
- <sup>16</sup>E. Domany, D. Mukamel, and A. Schwimmer, *J. Phys. A* **13**, L311 (1980).
- <sup>17</sup>O. Borisenko, G. Cortese, R. Fiore, M. Gravina, and A. Papa, *Phys. Rev. E* **83**, 041120 (2011).
- <sup>18</sup>A. B. Harris, *J. Phys. C* **7**, 1671 (1974).
- <sup>19</sup>S. Chen, A. M. Ferrenberg, and D. P. Landau, *Phys. Rev. Lett.* **69**, 1213 (1992).
- <sup>20</sup>J. J. Alonso, *J. Magn. Magn. Mater.* **322**, 1330 (2010).
- <sup>21</sup>S. A. Leonel, P. Z. Coura, A. R. Pereira, L. A. S. Mol, and B. V. Costa, *Phys. Rev. B* **67**, 104426 (2003).
- <sup>22</sup>T. Surungan and Y. Okabe, *Phys. Rev. B* **71**, 184438 (2005).
- <sup>23</sup>G. M. Wysin, A. R. Pereira, I. A. Marques, S. A. Leonel, and P. Z. Coura, *Phys. Rev. B* **72**, 094418 (2005).
- <sup>24</sup>S. E. Korshunov, *Phys. Rev. B* **46**, 6615 (1992).
- <sup>25</sup>U. Wolff, *Phys. Rev. Lett.* **62**, 361 (1989).
- <sup>26</sup>J. S. Wang and R. H. Swendsen, *Physica A* **167**, 565 (1990).
- <sup>27</sup>P. Minnhagen and B. J. Kim, *Phys. Rev. B* **67**, 172509 (2003).